Biosensors and Bioelectronics 68 (2015) 55–61

Contents lists available at ScienceDirect

Biosensors and Bioelectronics

journal homepage: www.elsevier.com/locate/bios

Single electrode biosensor for simultaneous determination of interferon gamma and lysozyme

Jianfei Xia, Daimin Song, Zonghua Wang *, Feifei Zhang, Min Yang, Rijun Gui, Lin Xia, Sai Bi, Yanzhi Xia, Yanhui Li, Linhua Xia

Laboratory of Fiber Materials and Modern Textile, The Growing Base for State Key Laboratory, College of Chemical Science and Engineering, Shandong Sino-Japanese Center for Collaborative Research of Carbon Nanomaterials, Collaborative Innovation Center for Marine Biomass Fiber Materials and Textiles, Qingdao University, Qingdao, Shandong 266071, China

ARTICLE INFO

Article history:
Received 15 October 2014
Received in revised form
17 December 2014
Accepted 20 December 2014
Available online 23 December 2014

Keywords:
Biosensor
Lysozyme
Interferon gamma
Signal-on
Signal-off
Electrochemical

ABSTRACT

Simultaneous detection of multiple biomarkers holds great promise for acute leukemia evaluation. Here, a novel biosensor is developed for simultaneous electrochemical detection of interferon gamma (IFN-γ) and lysozyme (Lys) based on aptamer recognition by coupling "signal-on" and "signal-off" modes. On one Au electrode, two kinds of signaling probes labeled by the thiolated ferrocene (Fc)- and methy blue (MB)- were designed to hybridize with IFN-γ and Lys aptamers respectively to form partial complementary DNA duplexes. In the presence of IFN-γ and Lys, the target–aptamer interaction led to the release of aptamer from duplex DNA structure. The single-stranded signaling probes thus suffered from the conformation changes, which resulted in the decreased (or increased) oxidation peak current of Fc (or MB) according to the "signal-off (or signal-on)" mode. Electrodes were characterized using cyclic voltammetry (CV) and electrochemical impedance spectroscopy (EIS). Under the optimized conditions, the signal changes were quantified using square wave voltammetry (SWV). This proposed biosensor for IFN-γ and Lys possessed linear detection range from 0.01 to 10 nM and 0.1 to 100 nM, with the detection limits of 1.14×10^{-3} nM and 0.0164 nM, respectively. Moreover, this biosensor was readily regenerated and proved successful toward the practical analysis. The proposed strategy could provide more integrated and reliable information for acute leukemia evaluation.

1. Introduction

Acute leukemia is one of the commonest cancer affecting children, and is a major cause of morbidity in hematopoietic cancer adults (Mullighan and Downing, 2009). The chances of survival for patients could be improved enormously if the disease was diagnosed and classified comprehensively. Identifying the content variations of the related analytes at the ultralow level has great value in understanding the immunity of the patients and the classification of the disease, which is becoming increasingly imperative for cancer detection, prevention, and therapy (Espina et al., 2005; Hanahan and Weinberg, 2000). Lysozyme (Lys) and interferon gamma (IFN-γ) are important analytes related to acute leukemia. Although they are often overproduced in several other diseases (e.g. rheumatoid arthritis, Torsteinsdóttir et al., 1999; tuberculosis, Wongtim et al., 1999; etc.), they have been proved useful in the classification and evaluation of the acute leukemia. The changes of Lys can be used to distinguish between subtypes (such as acute promyelocytic leukemia and acute myelomonocytic leukemina) (Sexton et al., 1996; Astrom et al., 2003). And the concentration of IFN-γ reflects the cellular immune level and the body's immue function of patients (Brady et al., 2011). Therefore, from a practical (time and cost) point of view, development of a dual biosensor with the ability of detecting Lys and IFN-γ simultaneously is broadly valuable in facilitating more efficient diagnosis.

For more progressive diagnosis, a much higher sensitivity is needed. An ideal dual biosensor should be able to provide the ability to detect the two analytes simultaneously, while keeping the increase of complexity and the sacrifice of accuracy to a minimum. Electrochemical analysis has the advantages of high sensitivity, compatibility for miniaturization, easy operation and low cost, making it an attractive candidate for two biomarkers testing systems (Wang, 2002; Lee and Hsing, 2006). However, the vast majority of reports are concerned with the detection of only single analyte (for Lys, Jing et al., 2010; Subramanian et al., 2013; Lian et al., 2014; Erdema et al., 2014; for IFN-γ, Chang et al., 2012; Chen et al., 2014; Zhang et al., 2012; Zhao et al., 2012; Jiang et al.,

* Corresponding author. Fax: +86 532 85950873. wangzonghua@qdu.edu.cn, 13853219173@126.com

http://dx.doi.org/10.1016/j.bios.2014.12.045
0956-5663/

2013). In recent years, some truly multiplexed examples have been presented for simultaneous detection of two different analytes. For example, Xu et al. (2014) proposed a sandwitch-format electrochemical immunosensor for the simultaneous detection of two tumor markers (carcinoembryonic antigen (CEA) and alpha-fetoprotein (AFP)). Qi et al. (2012) developed an electrochemical immunoassay array for the simultaneous detection of CEA and AFP by incorporating electrochemically addressing immobilization and one signal antibody strategy. Luo et al. (2014) presented the use of thermally cross-linked poly (ethylene glycol) polymer sensory array interfaces for the ultrasensitive quantification of two protein markers (insulin and C-reactive protein). However, to the best of our knowledge, so far no related work has been reported on the development of a simple and reusable dual biosensor with the aim of simultaneous determination of Lys and IFN-γ.

Aptamers hold great promise for the biosensing of disease-related analytes (Mayer, 2009). To realize the multiplex detection on a single working electrode, the ideal of which is to label different signaling probes with different indicators that produce signals at different potentials and monitor the decreased or increased oxidation–reduction peak current of the electroactive labels, known as "signal-off" and "signal-on" modes. Either the "signal-off" or "signal-on" sensor has become one of the most promising DNA sensors due to their various merits including high sensitivity and selectivity, as well as the reagentless and reusable advantages (Farjami et al., 2011; Qian et al., 2014, 2015). Furthermore, considering that the biosensors based on the structural switching of the redox-tagged aptamers might suffer from the limitation in sensor regeneration owing to the strong binding affinity of aptamers to targets (Liu et al., 2010; Chen et al., 2013; Cheng et al., 2007; Radi et al., 2006), the aptamer–DNA duplexes have been used in the biosensor architectures (Peng et al., 2009).

By combining the advantages of aptamer recognition and electrochemical "signal-off" and "signal-on" modes, a sensitive and selective dual biosensor was established for the simultaneous determination of IFN-γ and Lys, aiming to realize the integrated and classified diagnosis of the acute leukemia. Electrodes were easily fabricated and characterized using cyclic voltammetry (CV) and electrochemical impedance spectroscopy (EIS). Under the optimized conditions, the change in the redox current was quantified using square wave voltammetry (SWV). Furthermore, the biosensor can be readily regenerated and proved successful in practical sample analysis. This biosensor provides a specific and sensitive method for simultaneous detecting two analytes related to acute leukemia, exhibiting a great applied potential in clinical analysis.

2. Experimental section

2.1. Reagents and materials

The underlined bases in signaling probes and aptamers are complementary to form the partial complementary DNA duplexes. IFN-γ aptamer (A-IFN-γ): 5′-GGG GTT GGT TGT GTT GGG TGT TGT GTC CAA CCC C-3′ (Liu et al., 2010); Fc-modified IFN-γ signaling probe (P-Fc): 5′-SH-C6-TTA ACA CAA CTT TTT TTT TTG ACA CAA CAT-Fc-3′; Lys aptamer (A-Lys): 5′-ATC AGG GCT AAA GAG TGC AGA GTT ACT TAG-3′ (Cox and Ellington, 2001; Huang et al., 2010) and MB-modified Lys signaling probe (P-MB): 5′-SH-C6-*GTG CAG AGC TAA GTA ACT CTG CAC*-MB-3′ (the italic bases are complementary so that P-MB can fold into a hairpin configuration). All oligonucleotides were obtained from Sangon Biotechnol. Co. Ltd. (Shanghai, Chain), and were HPLC-purified and freeze-dried.

Immunoglobulin G (IgG) and 6-mercaptohexanol (MCH) were purchased from Aladdin. Recombinant human IFN-γ, Lys, thrombin (Thrb), bovine serum albumin (BSA), bovine serum hemoglobin (BHb) and Tris-(2-carboxyethyl) phosphine hydrochloride (TCEP) were obtained from Sangon Biotech (Shanghai) Co., Ltd. Recombinant human IL-6 and recombinant human PDGF-BB were purchased from GL Biochem (Shanghai), Ltd. Tris(hydroxymethyl) aminomethane (Tris) and NaCl were purchased from Shanghai AIBI Chemistry Preparation Co., Ltd. All other reagents are of analytical grade and used as received.

2.2. Apparatus

Electrochemical measurements were performed at room temperature on a CHI-660C electrochemical workstation (Shanghai Chenhua Instrument Co., Ltd., China) using a common three-electrode configuration where DNA probe-modified Au electrodes were used as working electrodes, platinum wire as an auxiliary electrode and saturated calomel as a reference electrode (SCE).

2.3. Biosensor preparation

Au electrode was firstly polished to show a mirror-like surface with 0.3 μm wet alumina slurries and rinsed repeatedly with water, followed by ultrasonication in ethanol and water. Subsequently, the polished electrode was voltammetrically cycled in 0.5 M H_2SO_4 aqueous solution with the potential of 0.2–1.65 V at the scan rate of 100 mV/s until the achievement of cyclic voltammogram characteristic for the clean Au electrode. Then, the electrode was washed thoroughly with enough amounts of water, and dried under N_2 atmosphere. Finally, DNA duplex was immobilized onto the pre-cleaned electrode to fabricate the biosensor.

The DNA duplex was firstly prepared as follows: signaling probe was dissolved in 100 mM Tris–HCl buffer (100 mM NaCl and 10 mM TCEP, pH 7.4) and incubated in the dark for 1 h to reduce disulfide bonds. Then, 10 μM of signaling probe solution was added to 10 μM of aptamer solution (100 mM Tris–HCl buffer, 100 mM NaCl and 1 mM $MgCl_2$, pH 7.4). The solution was then diluted to achieve a concentration of 1 μM for each oligonucleotide. After that, the mixture was heated to 90 °C keeping for 5 min, and then gradually cooled to room temperature and further incubated for 2 h at 37 °C to form DNA duplex. Afterwards, the pre-cleaned Au electrode was incubated in DNA duplex solution (1 μM P-Fc-A-IFN-γ or 1 μM P-MB-A-Lys or the mixture of 1 μM P-Fc-A-IFN-γ and 1 μM P-MB-A-Lys) (The choice of ds-DNA immobilization concentration is shown in Fig. S1) for 20 h at room temperature to obtain the modified electrodes (P-Fc-A-IFN-γ/Au or P-MB-A-Lys/Au or P-Fc-A-IFN-γ-P-MB-A-Lys/Au). After the modification, the electrodes were rinsed with washing buffer solution (10 mM Tris–HCl, pH 7.4) and further passivated with 1 mM MCH solution (in 10 mM Tris–HCl) for 1 h to block the uncovered Au electrodes surface. The electrodes were rinsed again with water and then washing buffer.

To monitor the each step for immobilization, the measurements of EIS and CV were performed in 0.1 M of KCl aqueous solution containing 5 mM of $[Fe(CN)_6]^{3-/4-}$ as the probe. EIS was performed in the frequency range of 0.01–100 kHz, together with 5 mV as the frequency modulation. CV measurements were recorded with a step potential of 1 mV in the potential range of –0.8 to 1.0 V at a scan rate of 100 mV/s.

2.4. Electrochemical detection of lysozyme and interferon gamma

In a typical detection process, the modified electrode was incubated in 50 μL target (Lys or IFN-γ or the mixture of Lys and IFN-γ) of different concentrations in 100 mM of Tris–HCl (containing 100 mM NaCl and 1 mM $MgCl_2$, pH 7.4) at 37 °C for 80 min. The

unbinding targets were removed by rinsing with water and washing buffer. The electrode was further immersed in a solution with high ionic strength (100 mM Tris–HCl containing 140 mM NaCl and 5 mM $MgCl_2$, pH 7.4) for 30 min at room temperature. Then, the resulting electrode was employed as the biosensor and investigated by SWV under a step potential of 4 mV, a frequency of 25 Hz, and an amplitude of 25 mV by scanning the potential from −0.5 to 0.5 V in 10 mL of 100 mM Tris–HCl (containing 140 mM NaCl, 5 mM $MgCl_2$, pH 7.4). The concentration of IFN-γ or Lys were quantified by calculating the change of averaged oxidation peak currents (ΔI) over five selected working electrodes ($\Delta I_{Lys}=I-I_o$ for Lys, $\Delta I_\gamma=I_o-I$ for IFN-γ, where I_o and I are the Fc- and MB-oxidation peak currents before and after the IFN-γ or Lys binding interactions, respectively).

2.5. Biosensor regeneration

After the detection, the electrode was regenerated by incubation in 2 μM aptamer solution (100 mM Tris–HCl, 100 mM NaCl, 1 mM $MgCl_2$, pH 7.4) for 2 h. After the washing treatment, the regenerated electrode became available for another assay.

3. Result and discussion

3.1. Sensing mechanism of the biosensor

The sensor architecture and signaling mechanism are shown in Scheme 1. In brief, the sensor involves the co-immobilization of two partial complementary DNA duplexes onto a Au electrode by using the thiol-gold chemistry. One duplex consists of P-Fc and A-IFN-γ, where Fc is used to produce electrochemical signals. Two aptamer recognition regions of P-Fc at its 3′- and 5′-ends are connected by a 10-thymine (T) spacer, which allows a better controlling for the spacer length and flexibility; and two addional T(s) at the 5′-end to improve probe flexibility (Wu and Lai, 2013). The hybridization of A-IFN-γ (the three bases between the two binding domains could add flexibility and enhance the hybridization) with the two regions brings together the two domains of P-Fc to form a "closed" structure that confines Fc approaching to the electrode surface for efficient electron transfer. In the presence of target IFN-γ, A-IFN-γ departs from the duplex as a result of the formation of the aptamer-IFN-γ bioaffinity complex. Meanwhile, the P-Fc is highly flexible and thus makes the "closed" structure opened, accompanying with a relatively far distance between Fc and the electrode surface. This change can result in a decrease in the electron transfer of Fc, reflecting in a "turn-off" signal. The other one of duplex consists of P-MB and A-Lys, where MB is used as the electroactive molecules. The 8-bp-long loop of P-MB was long enough to ensure that A-Lys hybridization affinity would be stronger than P-MB self-hybridization. Meanwhile the 8-bp-long loop of P-MB would not restrict the aptamer/target binding in the presence of Lys. In addition, the 8-bp-long stem was designed to make certain that the hairpin structure would form once aptamer/target binding had occurred (Huang et al., 2010). In the absence of target Lys, A-Lys hybridizes with part (the loop region and one stem) of the P-MB. The rigid construction of the forming DNA duplex prevents MB from accessing the electrode surface for efficient electron transfer. However, upon the target binding, DNA duplex is disrupted and A-Lys dissociates from DNA duplex into solution. Subsequently, the remaining P-MB with tailor made complementary bases at the both ends forming a hairpin structure, which brings the MB closing to the electrode surface. As a result, the electron transfer of MB is facilitated, together with the "turn-on" signal. Generally, the current decreased (or increased) degree is related to the concentration of IFN-γ (or Lys). Thus, the changes in peak currents of Fc and MB can be used as signals for quantitation of IFN-γ and Lys.

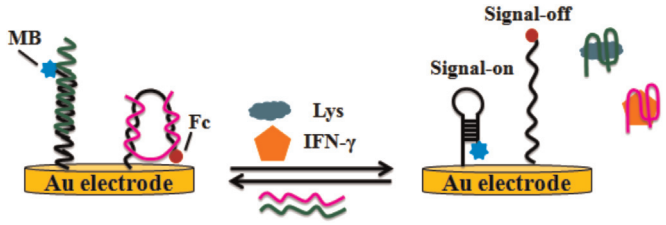

Scheme 1. Schematic representation of working principle of the "signal-on" and "signal-off" modes of the dual biosensor .

3.2. Characterization of biosensor

CV and EIS were employed for monitoring the each-step fabrication process of the biosensor (Fig. S2). As expected, at the bare Au electrode, the $[Fe(CN)_6]^{3-/4-}$ redox couple showed a minimal peak-to-peak separation (ΔE_p) (Fig. S1A–C, curve a). After the P-Fc-A-IFN-γ (or P-MB-A-Lys) (1 μM for each) was immobilized onto the Au electrode, the electrode exhibited a significant increase in the ΔE_p (192 mV and 149 mV, respectively) (Fig. S1A, curve b and Fig. S1B, curve b), which is due to the fact that the DNA duplex bears negative charges on its phosphate backbone, and produces electrostatic repulsive forces to the negatively charged probe anions $[Fe(CN)_6]^{3-/4-}$. The increased ΔE_p indicates that the double-stranded DNA (ds-DNA) is immobilized on the electrode. After the P-Fc-A-IFN-γ/Au (or P-MB-A-Lys/Au) was immersed in 10 nM IFN-γ (or 100 nM Lys), the DNA duplex denatured and liberated the aptamer into the solution, thus decreasing the kinetics barrier between $[Fe(CN)_6]^{3-/4-}$ and negatively charged phosphate backbones, together with a decreased ΔE_p value of 177 mV and 125 mV, respectively (Fig. S1A, curve c and Fig. S1B, curve c). When the electrode was modified with both 1 μM P-Fc-A-IFN-γ and 1 μM P-MB-A-Lys, the ΔE_p value markedly increased to 353 mV (Fig. S1C, curve b), which is larger than that of the ds-DNA immobilized separately. It is probably due to more ds-DNA immobilized essentially increased kinetics barrier between $[Fe(CN)_6]^{3-/4-}$ and the negatively charged phosphate backbones. After immersed in the target mixture (10 nM of IFN-γ and 100 nM of Lys), the ΔE_p value decresed to 280 mV (Fig. S1C, curve c), reasonably indicating that the designed biosensor has a potential for the simultaneous detection of IFN-γ and Lys. EIS further confirmed the above process (Fig. S1A′–C′). All experimental results demonstrated that the sensing interface had been successfully fabricated.

3.3. Feasibility of the biosensor

To evaluate the feasibility of this electrochemical assay, the single-analyte sensing was firstly performed using SWV. As shown in Fig. 1A, the voltammogram (obtained from P-Fc-A-IFN-γ/Au) presents the well shaped peak current at 275 mV (curve a). After the treatment with 10 nM of IFN-γ, the decreased peak current was observed without its position change (curve b). Fig. 1B illustrates that only a very low and broad peak at about −292 mV was observed on the P-MB-A-Lys/Au (curve a). After the electrode was immersed in 100 nM of Lys, the increased peak current with unchanged position was observed (curve b). These results adequately indicate the feasibility of this proposed assay.

Notably, the P-MB acts as a conventional "signal-on" probe in our biosensor, where the P-Fc functions as a "signal-off" probe. On the basis of the literature data, both types of signal generations ("signal-on" and "signal-off") are related to the length difference of

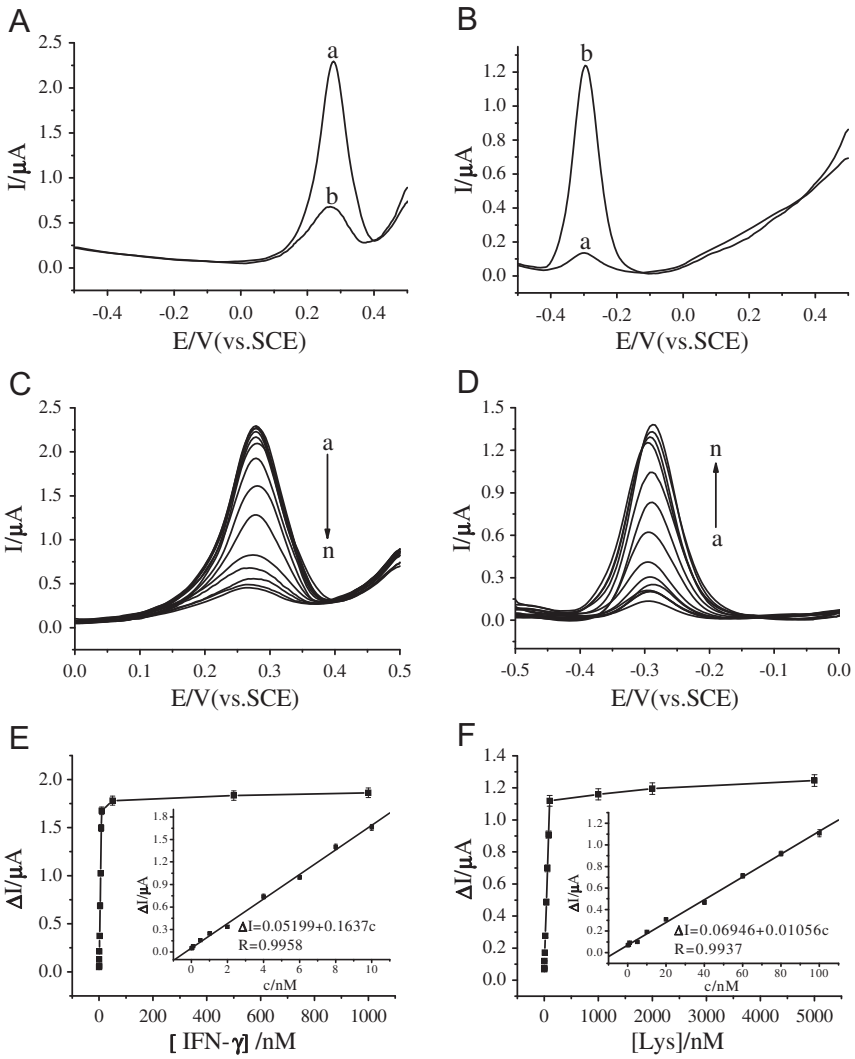

Fig. 1. SWVs of electrodes: (A) P-Fc-A-IFN-γ/Au (curve a) and after interaction with 10 nM IFN-γ (curve b); (B) P-MB-A-Lys/Au (curve a) and after interaction with 100 nM Lys (curve b); (C) P-Fc-A-IFN-γ/Au interaction with different concentrations of IFN-γ (curves a–n: 0–1000 nM); (D) P-MB-A-Lys/Au interaction with different concentrations of Lys (curves a–n: 0–5000 nM) in 100 mM Tris–HCl (140 mM NaCl, 5 mM $MgCl_2$, pH 7.4). The relationships between peak currents for (E) P-Fc-A-IFN-γ/Au and IFN-γ concentrations; (F) P-MB-A-Lys/Au and Lys concentrations. Insert: calibration curve for IFN-γ and Lys, respectively.

probes. The conformational change in a Fc-modified 15-base aptamer binding thrombin caused the increased redox probe current, corresponding to the "signal-on" mode (Sánchez et al., 2006). Oppositely, the "signal-off" mode was reported as the thrombin was bound to the MB-modified 32-base aptamer (Xiao et al., 2005). Obviously, the longer and shorter base oligoribonucleotides are respectively inclined to be involved in "signal-off" and "signal-on" modes. Accordingly, in our work, the P-Fc is 30-base in length, and generated the signal based on a "signal-off" mode, while the P-MB with 24-bases is designed to be employed in a "signal-on" mode.

Then, the single-analyte sensing was performed to assess the system sensitivity toward targets. We tested the response of each electrode (P-Fc-A-IFN-γ/Au or P-MB-A-Lys/Au) to the respective target (IFN-γ or Lys) of different concentrations. The relevant results are presented in Fig. 1C and D. Both electrodes responded to respective targets in a concentration-dependent manner. As shown in Fig. 1E, the peak currents (ΔI) fits the linear equation of $\Delta I_\gamma = 0.05199 + 0.1637c$ ($R = 0.9958$) when the concentrations of IFN-γ are in the range of 0.01–10 nM. The limit of detection (LOD) for IFN-γ is evaluated to be 1.09×10^{-3} nM (a signal-to-noise ratio (S/N) $= 3$). Similarly, as shown in Fig. 1F, the linear range of Lys is from 0.1 to 100 nM with a regression equation of $\Delta I_{Lys} = 0.06946 + 0.01056c$ ($R = 0.9937$) and a detection limit of 0.0158 nM ($S/N = 3$). Some differences in the sensitivity could be originated from the different density of probes on the electrode surface and the different dissociation constants (K_D) of target–aptamer complex dissociating into free target in solution for the IFN-γ (0.311 nM) (Liu et al., 2010) and Lys (31 nM) (Huang et al., 2010). It also could be found that when the IFN-γ concentration increased to 10 nM and Lys concentration increased to 100 nM or higher, the peak current signal tended to level off, suggesting the saturation of sensing surface.

A comparison of the proposed biosensor with other electrochemical IFN-γ and Lys biosensor is listed in Table 1. It can be seen that the LOD of our proposed sensor is lower than most of the previously reported sensors.

3.4. Optimization of experimental conditions

Experimental conditions (such as the incubation conditions) that affecting the biosensor performance were optimized by ananlyzing 8 nM IFN-γ and 80 nM Lys. Once one parameter was changed, the other parameters were fixed at the optimal values. The results are shown in the Supplementary materials (Fig. S3). The optimal incubation of this experiment was carried out in

Table 1
A comparision between the proposed assay and other reported techniques for the determination of (A) IFN-γ and (B) Lys.

Method	Technique	LOD (nM)	Linear range (nM)	Reference
(A)				
Electrochemical	DPV[a]	6.5×10^{-5}	1.0×10^{-4}–7.0×10^{-4}	Yan et al. (2013)
Electrochemical	SWV	1.09×10^{-3}	0.01–10	This work
Electrochemical	SWV	0.06	0.06–10	Liu et al. (2010)
Electrochemical	SWV	0.06	0.06–11.8	Liu et al. (2011)
Electrochemical	SWV	0.077	0.06–29.6	Chen et al. (2014)
Electrochemical	CV	0.1	0.1–10	Zhang et al. (2012)
Electrochemical	DPV	0.3	0.5–300	Zhao et al. (2012)
(B)				
Electrochemical	DPV	2.0×10^{-5}	6.8×10^{-5}–3.4×10^{-3}	Xie et al. (2014)
Electrochemical	SWV	1.0×10^{-4}	1.0×10^{-4}–10	Chen et al. (2013)
Electrochemical	SWV	0.0158	0.1–100	This work
Electrochemical	FIS[b]	0.07	0.2–4	Peng et al. (2009)
Electrochemical	SWV	0.45	7–30	Chen and Guo (2013)
Electrochemical	SPQC[c]	0.5	0.5–100	Lian et al. (2014)
Electrochemical	EIS	28.53	30–68	Erdema et al. (2014)

[a] Differential pulse voltammetry.
[b] Faradic impedance spectroscopy.
[c] Series with piezoelectric quartz crystal.

100 mM Tris–HCl (pH 7.4) containing 100 mM Na^+ and 1.0 mM Mg^{2+} for 80 min at 37 °C.

3.5. Selective and simultaneous determination of IFN-γ and Lys

Firstly, to prove the two targets (IFN-γ and Lys) can be selectively detected, the P-Fc-A-IFN-γ-P-MB-A-Lys/Au was treated with IFN-γ and Lys in sequence. In the absence of targets, a well shaped peak current (at 275 mV), a low and broad peak (at −292 mV) were observed (Fig. S4A, black curve). When 10 nM of IFN-γ was added in the solution, the peak current at 275 mV decreased while that at −292 mV remained unchanged (Fig. S4A, red curve). Adding 100 nM of Lys to the solution continuously, the peak current at −292 mV increased while that at 275 mV remained as the last step (Fig. S4A, blue curve). Reversing the sequence of added targets (100 nM of Lys and then 10 nM of IFN-γ), the results in Fig. S4B (red and blue curves) illustrate that the peak current at −292 mV firstly increased when Lys was added, while it kept steady after IFN-γ was added. However, the peak current at 275 mV performed oppositely. Furthermore, the position of two observed peaks in these experiments were the same as that in the previous experiment, indicating that the prepared dual biosensor is capable of responding to the each one of targets selectively.

In the second step, to prove the IFN-γ and Lys that can be simultaneously detected, the P-Fc-A-IFN-γ-P-MB-A-Lys/Au was stimulated with a mixture of the two targets. Representative results are presented in Fig. 2A. The changes of peak current have the same tendency as the case of using the single target. The peak currents of IFN-γ decreased and that of Lys increased with their concentrations increase. As shown in Fig. 2B, the ΔI_γ and ΔI_{Lys} were in the linear relationship to the concentrations of IFN-γ (line a) and Lys (line b) in the detected range with regression equations of $\Delta I_\gamma = 0.06187 + 0.1473c$ ($R = 0.9972$) and $\Delta I_{Lys} = 0.04455 + 0.00993c$ ($R = 0.9973$). The detection limits were 1.14×10^{-3} nM and 0.0164 nM, respectively. Therefore, the proposed analytical system containing a single electrode is suitable for the simultaneous detection of IFN-γ and Lys.

3.6. Specificity and practical applicability

Specificity is a critical issue in the development of the biosensors for applications in biomedical systems. The specificity test was carried out by measuring and comparing the response of 10 nM IFN-γ and 100 nM Lys to some nonspecific interferential biomolecules including BSA, BHb, Thrb, IgG, PDGF-BB, IL-6 and their mixture with higher concentrations (2 μM). As shown in Fig. S5, the peak current intensity of IFN-γ and Lys was much higher than those of the other interferential biomolecules which did not bind to the aptamer. In addition, the assay also showed good response to targets in the mixture of the proteins. And the non-additive nature of the signals was observed for interfering biomolecules. These results indicated that our biosensor was able to recognize IFN-γ and Lys as the targets with high specificity.

To evaluate the applicability and reliability of the proposed

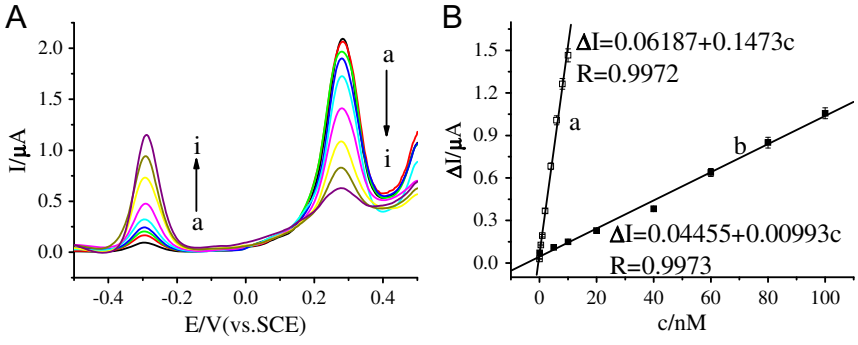

Fig. 2. (A) SWVs of P-Fc-A-IFN-γ-P-MB-A-Lys/Au (curve a) and after interaction with different concentrations (curves b–i) of IFN-γ (0.01–10 nM) and Lys (0.1–100 nM) in 100 mM Tris–HCl (140 mM NaCl, 5 mM $MgCl_2$, pH 7.4). (B) The calibration curves for IFN-γ (curve a) and Lys (curve b).

Table 2
Results of determination of IFN-γ and Lys in the 300-fold-diluted human serum samples.

	Samples	Detected (nM)	Added (nM)	Found (nM)	Recovery (%)	RSD[a] (%)
1	Lys	2.12	2.5	4.46	93.60	3.72
	IFN-γ	0	2.5	2.32	92.80	3.96
2	Lys	2.08	2.5	4.66	103.2	4.16
	IFN-γ	0	2.5	2.60	104.0	4.34
3	Lys	2.17	2.5	4.53	94.40	3.26
	IFN-γ	0	2.5	2.34	93.60	3.84
4	Lys	2.21	2.5	4.85	105.6	3.78
	IFN-γ	0	2.5	2.39	95.60	4.32

[a] The results listed in the table were obtained from five independent experiments.

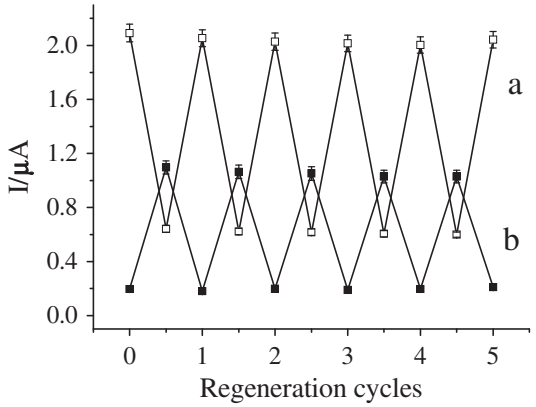

Fig. 3. Regeneration of the aptasensor challenged with 10 nM IFN-γ (curve a) and 100 nM Lys (curve b) over five cycle uses. Data shown are average measurements from three different electrodes.

biosensor, the 300-fold-diluted human serum from healthy individuals was tested. Normal serum typically contains 1 pM IFN-γ (Chang et al., 2012), which is less than the detection limit. Standard solutions of IFN-γ and Lys were added and detected by the SWV measurements. Recoveries are shown in Table 2. According to the procedure of spiked standards, the spiked recoveries are 92.80–104.0% and 93.60–105.6% for IFN-γ and Lys, respectively. In the test, each sample underwent five parallel measurements, and the relative standard deviation (RSD) was below 5%, suggesting a good reproducibility. These results clearly indicate the applicability of the proposed method.

3.7. Regeneration and stability

Because the designed sensor was based on the target competing reaction between targets and part complementary strands, it can be regenerated through a simple procedure. As can be seen in Fig. 3, after five cycles of regeneration processes, the Fc (curve a) and MB (curve b) signals are both almost recovered to the original values, indicating the good regeneration ability of the developed biosensor.

The stability of this sensor was investigated by storing it at 4 °C and measuring once a day over a period of 3 weeks. As a result, the sensor remained bioactive. And only a small decrease of the oxidation peak current was observed (the signal changes were 4.57% for IFN-γ and 4.34% for Lys). The above results demonstrate that this proposed biosensor has a sufficient stability.

4. Conclusions

In summary, on the basis of aptamer recognition and electrochemical "signal-on" and "signal-off" modes, a novel dual biosensor was established for the simultaneous determination of two analytes (IFN-γ and Lys) related to acute leukemia. The proposed biosensor can be easily fabricated and readily regenerated, accompanying with high sensitivity (detection limits were 1.14×10^{-3} nM and 0.0164 nM for IFN-γ and Lys, respectively). Furthermore, this bosensor is resistant to the interferences from other proteins inherently and proved successful towards the practical analysis in human serum. This novel approach could offer more integrated and reliable information for the acute leukemia diagnosis, promoting the development of an effective and efficient evaluation of acute leukemia.

Acknowledgments

We greatly appreciate the financial support from the National Natural Science Foundation of China (21405086, 21475071, 21275082, 81102411 and 21203228), the National Key Basic Research Development Program of China (973 special preliminary study plan, Grant no. 2012CB722705), the Taishan Scholar Program of Shandong Province and the Natural Science Foundation of Qingdao (13-1-4-128-jch and 13-1-4-202-jch).

Appendix A. Supplementary material

Supplementary data associated with this article can be found in the online version at http://dx.doi.org/10.1016/j.bios.2014.12.045.

References

Astrom, M., Bodin, L., Hornsten, P., Wahlin, A., Tidefelt, U., 2003. Eur. J. Haematol. 70, 26–33.
Brady, M.T., Lee, J., Ferrone, S., Wang, E.S., Wetzler, M., 2011. Leuk. Res. 35, 275–277.
Chang, C.C., Lin, S.H., Lee, C.H., Chuang, T.L., Hsueh, P.R., Lai, H.C., Lin, C.W., 2012. Biosens. Bioelectron. 37, 68–74.
Chen, Y., Pui, T.S., Kongsuphol, P., Tang, K.C., Arya, S.K., 2014. Biosens. Bioelectron. 53, 257–262.
Chen, Z.B., Guo, J.X., 2013. Electrochim. Acta 11, 916–920.
Chen, Z.B., Guo, J.X., Li, J., Guo, L., 2013. RSC Adv. 3, 14385–14389.
Cheng, A.K.H., Ge, B.X., Yu, H.Z., 2007. Anal. Chem. 79, 5158–5164.
Cox, J.C., Ellington, A.D., 2001. Bioorg. Med. Chem. 9, 2525–2531.
Erdema, A., Eksina, E., Muti, M., 2014. Colloids Surf. B 115, 205–211.
Espina, V., Geho, D., Mehta, A.I., Petricoin, E.F., Liotta, L.A., Rosenblatt, K.P., 2005. Cancer Investig. 23, 36–46.
Farjami, E., Clima, L., Gothelf, K., Ferapontova, E.E., 2011. Anal. Chem. 83, 1594–1602.
Hanahan, D., Weinberg, R.A., 2000. Cell 100, 57–70.
Huang, J., Zhu, Z., Bamrungsap, S., Zhu, G.Z., You, M.X., He, X.X., Wang, K.M., Tan, W. H., 2010. Anal. Chem. 82, 10158–10163.
Jiang, J., He, Y., Yu, X.X., Zhao, J.Y., Cui, H., 2013. Anal. Chim. Acta 791, 60–64.
Jing, T., Du, H.R., Dai, Q., Xia, H., Niu, J.W., Hao, Q.L., Mei, S.R., Zhou, Y.K., 2010. Biosens. Bioelectron. 26, 301–306.
Lee, T.M.H., Hsing, I.M., 2006. Anal. Chim. Acta 556, 26–37.
Lian, Y., He, F.J., Mi, X.W., Tong, F.F., Shi, X.H., 2014. Sens. Actuators B 199, 377–383.
Liu, Y., Tuleouva, N., Ramanculov, E., Revzin, A., 2010. Anal. Chem. 82, 8131–8136.
Liu, Y., Yan, J., Howland, M.C., Kwa, T., Revzin, A., 2011. Anal. Chem. 83, 8286–8292.
Luo, X.L., Xu, Q., James, T., Davis, J.J., 2014. Anal. Chem. 86, 5553–5558.
Mayer, G., 2009. Angew. Chem. Int. Ed. 48, 2672–2689.
Mullighan, C.G., Downing, J.R., 2009. Leukemia 23, 1209–1218.
Peng, Y.G., Zhang, D.D., Li, Y., Qi, H.L., Gao, Q., Zhang, C.X., 2009. Biosens. Bioelectron. 25, 94–99.
Qi, H.L., Ling, C., Ma, Q.Y., Gao, Q., Zhang, C.X., 2012. Analyst 137, 393–399.
Qian, Y., Tang, D.Q., Du, L.L., Zhang, Y.Z., Zhang, L.X., Gao, F.L., 2015. Biosens. Bioelectron. 64, 177–181.

Qian, Y., Wang, C.Y., Gao, F.L., 2014. Talanta 130, 33–38.
Radi, A.E., Sánchez, J.L.A., Baldrich, E., O'Sullivan, C.K., 2006. J. Am. Chem. Soc. 128, 117–124.
Sánchez, J.L.A., Baldrich, E., Radi, A.E.G., Dondapati, S., Sánchez, P.L., Katakis, I., O'Sullivan, C.K., 2006. Electroanalysis 18, 1957–1962.
Sexton, C., Buss, D., Powell, B., O'Connor, M., Rainer, R., Woodruff, R., Cruz, J., Pettenati, M., Rao, P.N., Case, L.D., 1996. Leuk. Res. 20, 467–472.
Subramanian, P., Lesniewski, A., Kaminska, I., Vlandas, A., Vasilescu, A., Jonsson, J.N., Pichonat, E., Happy, H., Boukherroub, R., Szunerits, S., 2013. Biosens. Bioelectron. 50, 239–243.
Torsteinsdóttir, I., Håkansson, L., Hällgren, R., Gudbjörnsson, B., Arvidson, N.G., Venge, P., 1999. Rheumatology 38, 1249–1254.
Wang, J., 2002. Anal. Chim. Acta 469, 63–71.
Wongtim, S., Silachamroon, U., Ruxrungtham, K., Udompanich, V., Limthongkul, S., Charoenlap, P., Nuchprayoon, C., 1999. Thorax 54, 921–924.
Wu, Y., Lai, R.Y., 2013. Chem. Commun. 49, 3422–3424.
Xiao, Y., Lubin, A.A., Heeger, A.J., Plaxco, K.W., 2005. Angew. Chem. Int. Ed. Engl. 44, 5456–5459.
Xie, D.P., Li, C.C., Li, S.G., Qi, H.L., Xue, D., Gao, Q., Zhang, C.X., 2014. Sens. Actuators B 192, 558–564.
Xu, T., Jia, X.L., Chen, X., Ma, Z.F., 2014. Biosens. Bioelectron. 56, 174–179.
Yan, G.P., Wang, Y.H., He, X.X., Wang, K.M., Liu, J.Q., Du, Y.D., 2013. Biosens. Bioelectron. 44, 57–63.
Zhang, H.X., Jiang, B.Y., Xiang, Y., Chai, Y.Q., Yuan, R., 2012. Analyst 137, 1020–1023.
Zhao, J.J., Chen, C.F., Zhang, L.L., Jiang, J.H., Yu, R.Q., 2012. Biosens. Bioelectron. 36, 129–134.